RSC Advances

PAPER

View Article Online
View Journal | View Issue

Cite this: *RSC Adv.*, 2019, **9**, 40772

Predicting viable isomers of [X,C,N] and [H,X,C,N] (X = Sn, Pb)†

Yu-Wang Sun,[a] Hai-Yan Wang*[ab] and Yi-Hong Ding *[a]

Received 30th October 2019
Accepted 1st December 2019

DOI: 10.1039/c9ra08943h

rsc.li/rsc-advances

Metal cyanide/isocyanide and hydrometal cyanide/isocyanide compounds are key metal-carriers in interstellar space. Lighter group 14 elements (X = C/Si/Ge) cyanides/isocyanides and hydrocyanides/hydroisocyanides have been studied theoretically and experimentally. However, no reports are available on the analogues of tin (Sn) and lead (Pb). In this work, we carried out the first theoretical study on the structures and stabilities of [X,C,N] and [H,X,C,N] (X = Sn/Pb) at the CCSD(T)/def2-QZVPP//B3LYP/def2-QZVPP level. Comparisons were made with the lower analogues (X = C/Si/Ge) concerning the structural, energetic and bonding properties. Significantly different from that of c-C_2N, a dative-bonded valence structure of c-XCN for heavier X was revealed for the first time, which can account for the rather worse kinetic stability of cyclic [X,C,N] for heavier X = Si/Ge. A unique kind of agostic bonding was found within three isomers of [H,Pb,C,N], whereas it is absent for X = C/Si/Ge/Sn. The computed structural and spectroscopic data could aid future laboratory and astrophysical detection of the [X,C,N] and [H,X,C,N] (X = Sn/Pb) isomers.

Introduction

Metals and metal-containing molecules are important constituents of the interstellar medium.[1] Understanding the structures and kinetics of these metal-containing species is crucial to metal chemistry in space. In particular, metal cyanides/isocyanides and hydrometal cyanides/isocyanides have been long viewed as major molecular carriers of metals in circumstellar gas, especially in IRC +10216. Up to now, a number of metal cyanide/isocyanide compounds have been detected in IRC +10216, *e.g.* MgNC, NaCN, MgCN, SiCN, AlNC, SiNC, KCN and FeCN.[2] By contrast, the hydrides of metal cyanides/isocyanides detected in space have been rather limited with only hydromagnesium isocyanide (HMgNC) now known.[3] Alternatively, theoretical results or/and experimental characterization have been reported for HSiCN/HSiNC, HGeCN/HGeNC, HZnCN/HZnNC, HFeCN/HFeNC and HTiCN/HTiNC systems in order to aid for their potential astrophysical detection.[4]

Tin (Sn) and lead (Pb) are among the earliest metals used by humans. Tin-containing compounds can be used as semiconductors, infrared nonlinear optical materials and organic light-emitting diodes at present.[5] Lead-containing compounds also have wide applications, *i.e.*, perovskite solar cells and solder.[6] And tin and lead can form intermetallic compounds with other metals, which have oscillatory superconducting properties, magnetic susceptibility and thermopower.[7] It has been previously shown that the kinetic and bonding evolution of the compounds containing the heavier group-14 elements can be significantly influenced by the periodic number and connected ligands.[8] However, the Sn/Pb-chemistry in space has received very little attention compared to the ample interest of Sn/Pb-chemistry on the earth. One possible reason could be ascribed to their much lower cosmic abundance than iron.[9] In spite of this, the detection report of Sn/Pb has continued to grow. In 1993, the 1400.450 Å line of Sn(II) was detected in the planetary nebulae (PNe) for the first time.[10] Two years later, the 1434 Å line of Pb(II) was also detected and scientists discovered three lead-rich stars (HD187861, HD196944 and HD224959) in 2001.[11] To our great surprise, theoretical and experimental investigations have not been reported for tin/lead cyanide/isocyanide and hydrotin/hydrolead cyanide/isocyanide, to the best of our knowledge. Those metal cyanide compounds could be present in C-rich circumstellar gas and provide important information about the species origin and their formation mechanism for the regions.

In the present work, we carried out the first theoretical study of the [X,C,N] and [H,X,C,N] (X = Sn/Pb) systems at the CCSD(T)/def2-QZVPP//B3LYP/def2-QZVPP level in both the low and high spin multiplicities. The detailed structural, thermodynamic and kinetic properties were analyzed in detail to allow for the detection in future laboratory and interstellar studies. We also compared [X,C,N] and [H,X,C,N] (X = Sn/Pb) with analogues of

[a]*Laboratory of Theoretical and Computational Chemistry, Institute of Theoretical Chemistry, Jilin University, Changchun 130023, P. R. China. E-mail: yhdd@jlu.edu.cn; jlsdwhy_0820@sina.cn*

[b]*College of Computer Science and Technology, Changchun University, Changchun 130023, P. R. China*

† Electronic supplementary information (ESI) available. See DOI: 10.1039/c9ra08943h

the same groups (X = C/Si/Ge) in regard to the structural, energetic and bonding properties.

Methods

All calculations were carried out with Gaussian09 program packages.[12] We used the locally developed global potential energy surface survey (GPESS) platform to build up the schematic plot of both isomers and transition states.[13] For search of isomers, we used the grid-based comprehensive isomeric search strategy[14] to construct the diversified initial structures at the B3LYP level with def2-SVP. For search of transition states, we applied the QST2-based algorithm.[15] Intrinsic reaction coordinate (IRC)[16] calculations were carried out to verify whether the transition state connects the correct isomers at the B3LYP/def2-SVP level. Subsequently, the isomers and transition states were re-optimized at B3LYP/def2-QZVPP level. Note that at both def2-SVP and def2-QZVPP-B3LYP levels, the stationary nature of each isomer and transition state was confirmed by the harmonic vibrational frequency calculations with the former possessing all positive frequencies whereas the latter only one imaginary frequency. The single-point energies with zero-point vibrational energy (ZPVE) correction were calculated at the CCSD(T)[17]/def2-QZVPP//B3LYP/def2-QZVPP level. In order to verify the reliability of CCSD(T)/def2-QZVPP//B3LYP/def2-QZVPP + ZPVE, we undertook the PBE0 [18]/def2-QZVPP optimizations followed by single-point CCSD(T)/def2-QZVPP energy calculations on the isomers of the doublet/quartet [X,C,N] and singlet/triplet [H,X,C,N] (X = Sn, Pb) (see Table S1 in the ESI†). It can be seen that based on all the values in Table S1,† the two types of calculations generally provide very similar predictions. The detailed flowchart of our GPESS study can be found in ESI.† Note that in the construction of [H,X,C,N] (X = Sn/Pb) potential energy surfaces (PES), the manual search was also conducted to remedy some difficulty cases that are very sensitive to the initial input structures.

It should be noted that the scalar relativistic effects were considered for the heavier metal atoms Sn and Pb through effective core potentials as described by the def series of basis sets.[19] The spin–orbit effects were not included. According to previous studies on the cyanides of group 1 and group 11 metal atoms, the spin–orbit effects on the spectroscopic properties can generally be not so large.[20] In addition, to discuss the bonding strength of the studied Sn/Pb-bearing isomers, we used the Mayer bond index analysis[21] throughout our study since the open-shell systems cannot be treated by the Wiberg bond index (WBI)[22] strategies. The atomic dipole moment corrected Hirshfeld (ADCH)[23] population analysis were computed by Multiwfn program.[24]

Results and discussions

The optimized structures of the isomers are shown in Fig. S1–S4,† respectively, while the vibrational frequencies of the isomers are given in Tables S5 and S6.† The energies of all the species are listed in Table S4.† Finally, the schematic potential energy surfaces (PES) of the doublet [X,C,N] (the PES of the quartet [X,C,N] are given in Fig. S5†) and singlet/triplet [H,X,C,N] (X = Sn/Pb) systems are plotted in Fig. 4–8. The symbol ^{s}**m** is used to describe an isomer of [Sn,C,N], [Pb,C,N], [H,Sn,C,N] or [H,Pb,C,N]. ^{s}**tsm/n** describes the interconversion transition state between the isomers ^{s}**m** and ^{s}**n**. The left superscript **s** denotes the spin multiplicity (1, 2, 3 and 4 for singlet, doublet, triplet, and quartet, respectively). Note that some processes were computed to have the negative barrier values, which are physically not meaningful and are the results of the higher-level single-point calculations at lower-level optimized geometries.

XCN ^{2}1, XNC ^{2}2, HXCN ^{1}1 and HXNC ^{1}2

The ground states for XCN/XNC and HXCN/HXNC (X = Sn/Pb) are doublet and singlet, respectively. For each of the systems, the former two lowest-energy isomers are XCN ^{2}**1**, XNC ^{2}**2**, HXCN ^{1}**1** and HXNC ^{1}**2**, respectively. Structurally (see Fig. 1), we can regard them as combinations of R (R = X/HX, X = Sn/Pb) and CN. Note that all the hydrides ^{1}**1** and ^{1}**2** are significantly bent with the very cute ∠HXC and ∠HXN angles of around 90°. This is due to the existence of the distinct electron lone pair at the X-atom, as frequently encountered in heavier group-14 compounds.[25]

From Si to Pb, the experimentally determined ionization potentials are 11.6, 8.1, 7.9, 7.3 and 7.0, respectively,[26] indicating the increased metallicity. This could be a result of the increasingly positive Hirshfeld and ADCH charges of X with increased periodic number (see Tables S2 and S3†). Yet, the trend of the NPA charges is not clear. In particular, for the hydride cyanide/isocyanides, the charge of hydrogen becomes increasingly negative for all the NPA, Hirshfeld and ADCH analysis, indicating that from Si to Pb, the hydrogen becomes more like an anion (H^-) rather than a proton.

Thermodynamically, it is interesting to find that the energy gaps between RNC and RNC (R = X and HX), *i.e.*, ΔE(XNC–XCN) and ΔE(HXNC–HXCN), are very similar to each other. The bonding interaction of R + CN/NC (R = X/HX; X = Si/Ge/Sn/Pb) as well as the Mayer bond index values get increasingly weaker (see Fig. 2 and 3).

Kinetically, the energy barriers for the conversion of ^{2}XNC to ^{2}XCN are 20.48, 13.79, 8.72, 1.74 kcal mol^{-1} for X = Si, Ge, Sn,

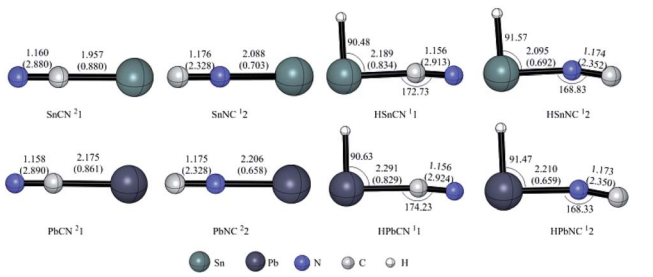

Fig. 1 Optimized geometries of isomers XCN ^{2}**1**, XNC ^{2}**2**, HXCN ^{1}**1** and HXNC ^{1}**2** (X = Sn, Pb) at the B3LYP/def2-QZVPP level. Bond lengths are in angstroms and angles are in degrees and the Mayer bond indices are in parentheses.

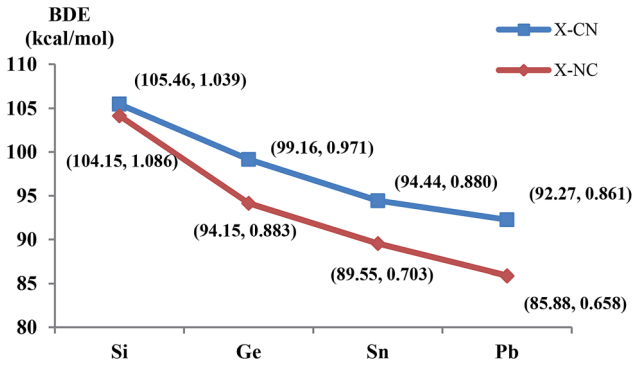

Fig. 2 The BDE and Mayer bond indices of X–CN and X–NC with the periodic increasing of X (X = Si/Ge/Sn/Pb), BDE(X–CN) = *E*(XCN) − *E*(X) − *E*(CN).

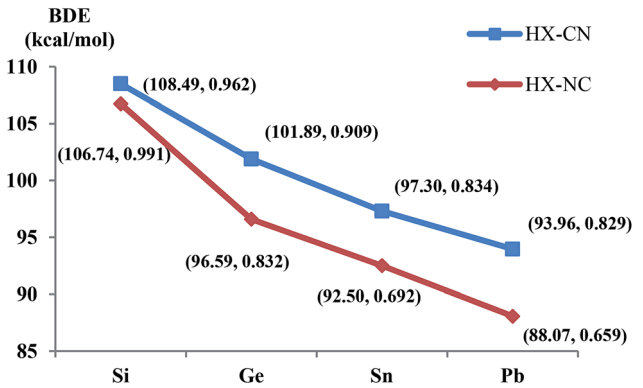

Fig. 3 The BDE and Mayer bond indices of HX–CN and HX-NC with the periodic increasing of X (X = Si/Ge/Sn/Pb), BDE(HX–CN) = *E*(HXCN) − *E*(HX) − *E*(CN).

Pb,respectively (see Fig. 4a and b). For R = HX (X = Si/Ge/Sn/Pb), such conversion barriers are 19.23, 13.24, 6.88 and 3.74 kcal mol^{-1}, respectively (see Fig. 5 and 6). Clearly, such ^{1}RNC → ^{1}RCN conversion barriers descend in a quite steep mode for X = Si, Ge, Sn, Pb with the increased metallic character of X. As shown in Fig. 7 and 8, the RNC → RCN conversion barriers are strongly correlated with the bonding energy of R–NC. The higher the bonding energy (R–NC) is, the higher the conversion barrier is. Due to the very large dissociation energies of RCN and RNC (R = X/HX, X = Sn/Pb) (92–97 kcal mol^{-1} towards R + CN; 58–68 kcal mol^{-1} towards H + XCN/XNC), we can optimistically expect their existence. Surely, with the lowered conversion barrier, RCN/RNC might have increased co-existing possibility.

We could not locate any cyclic [X,C,N] isomers for X = Sn/Pb on the lowest doublet PESs. We are aware that for the c-XCN → XCN/XNC conversion, the barrier (46.27/18.61 kcal mol^{-1}) is rather high for X = C,[27] whereas it is negligibly lower (6.64/1.73 and 1.13/0.53 kcal mol^{-1}) for X = Si/Ge.[28] Thus c-XCN is kinetically very unstable for all heavier X, contrasting X = C. What is the cause? We turned to the intrinsic valence structures of cyclic [X,C,N]. In the extensively studied c-C_2N, two identical C–N bonds contain significant multiple bonding and two equivalent resonance three-membered ring structures (see **I** in Fig. 11) have dominant contribution.[27b] In **I**, the radical-bearing carbon is also mainly associated with a C=N bond. Such fast-resonating structures are surely responsible for the good kinetic stability of c-C_2N. Among studies of the heavier elements X = Si/Ge,[29] we could not find any valence description for c-XCN. In this work, according to the bond distances, spin distribution and coordination analysis, we revealed a quite different valence structure **II** from c-C_2N. In **II**, multiple bonding is significantly localized with the C=N bond, whereas the unpaired spin is separately positioned on X-atom (see Table 1). Notably, the C–X in **II** is not a formal covalent bond. Instead, it is a dative bond due to the X → C donor–acceptor interaction. Besides, they might also exist the N → X dative interaction. Thus, it is the dative bond that accounts for the rather easy ring-opening of c-XCN (X = Si/Ge). The electron-donating and electron-accepting ability of X should both contribute to the stabilization of c-XCN. As shown by the binding energy of the model carbene H_2X with BH_3 and CO in Table 2, both abilities clearly decrease in the order of X = Si > Ge > Sn > Pb. Therefore, it's quite reasonable when X becomes the heavier Sn/Pb, the formal c-XCN isomer is not an energy minima.

HCNX ^{3}3, HCXN ^{3}4, HNCX ^{3}5 and HNXC ^{3}6

The ground state is triplet for the chainlike isomers HCNX **3** and HNCX **5**. They have similar cumulenic structural features, which can be considered as the intermolecular complexes that

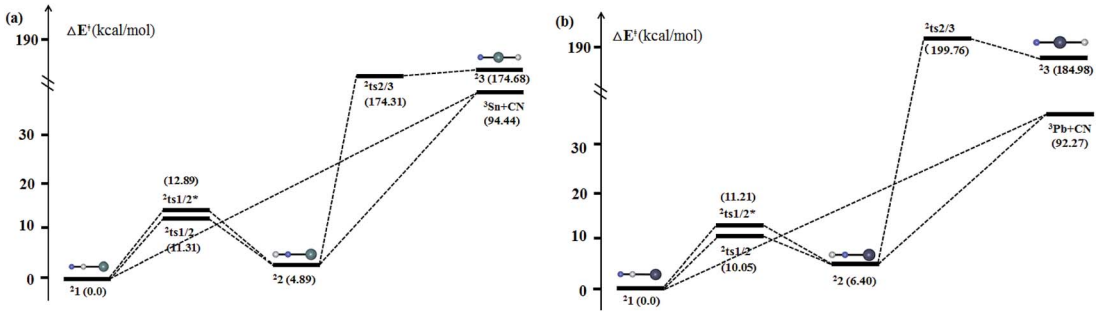

Fig. 4 (a) and (b) represent the schematic potential energy surfaces of doublet [X,C,N] of X = Sn and Pb, respectively. All the values are claculated at the level of CCSD(T)/def2-QZVPP//B3LYP/def2-QZVPP + ZPVE in the parenthesis.

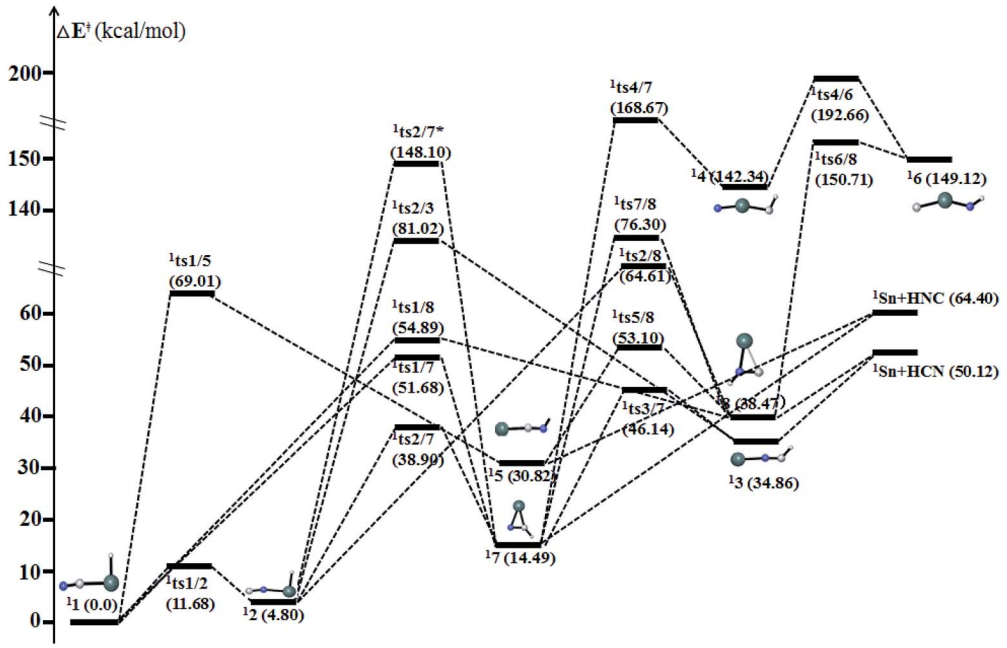

Fig. 5 Schematic potential energy surface of singlet [H,Sn,C,N] at the level of CCSD(T)/def2-QZVPP//B3LYP/def2-QZVPP + ZPVE in the parenthesis.

arise from the interaction between the X (X = Sn/Pb) atom and HCN/HNC at the N/C-ends (see Fig. 12). In fact, the dissociation of the N/C–X bonds to give the ^{3}X + HCN/HNC fragments should govern the kinetic stability of the isomer ^{3}**3**/^{3}**5**. Their dissociation energies 11.04/10.97 and 23.34/19.13 kcal mol^{-1} for X = Sn/Pb are considerably lower than the respective isomerization barriers (see Fig. 9 and 10). Clearly, the energetically more stable HCN is less reactive towards X than HNC. As a result, HCNX ^{3}**3** is much less chemically bounded than HNCX ^{3}**5**.

The chainlike isomers HCXN **4** and HNXC **6** also possess the triplet ground states. Both can be formally considered as the X-inserted structures of HCN/HNC (X = Sn/Pb) (see Fig. 12). They are reasonably very high-lying isomers at 137.57/147.84 and 131.81/139.91 kcal mol^{-1}, respectively, above HXCN ^{1}**1** (X = Sn/Pb). Despite the high energies of ^{3}**4**/^{3}**6**, their dissociation

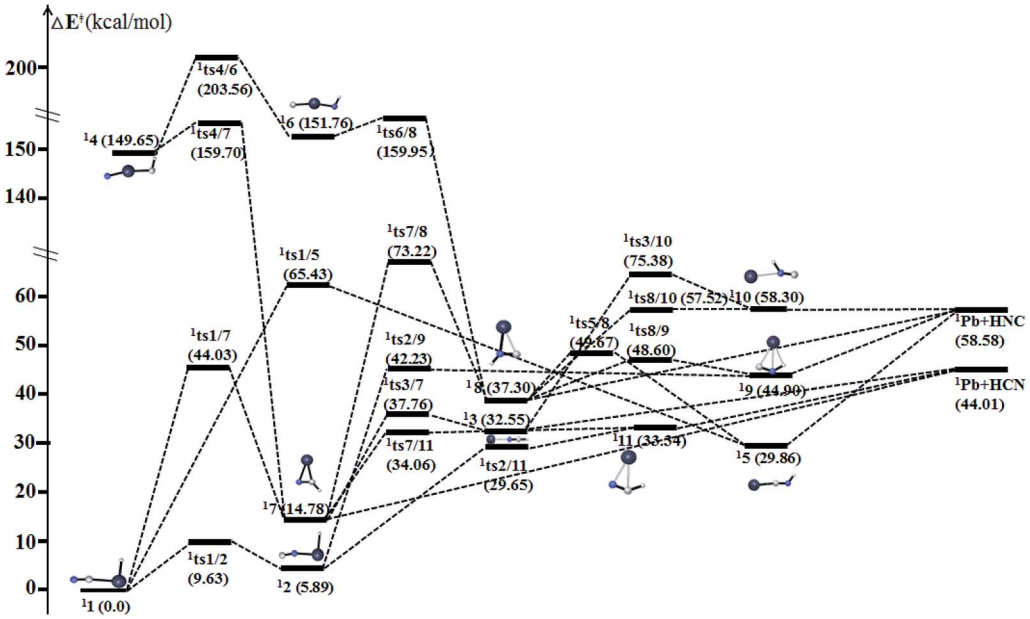

Fig. 6 Schematic potential energy surface of singlet [H,Pb,C,N] at the level of CCSD(T)/def2-QZVPP//B3LYP/def2-QZVPP + ZPVE in the parenthesis.

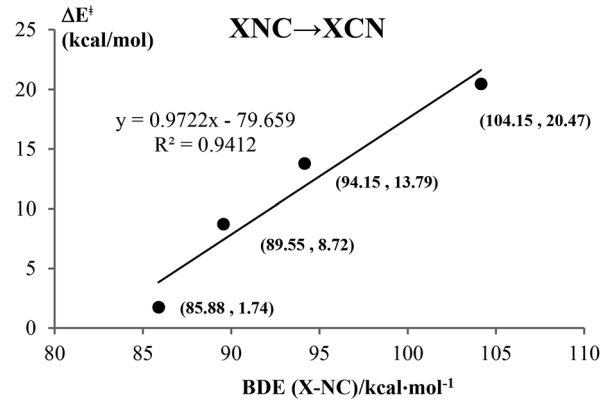

Fig. 7 The correlation between the bonding energies (X–NC) and the barriers (XNC → XCN).

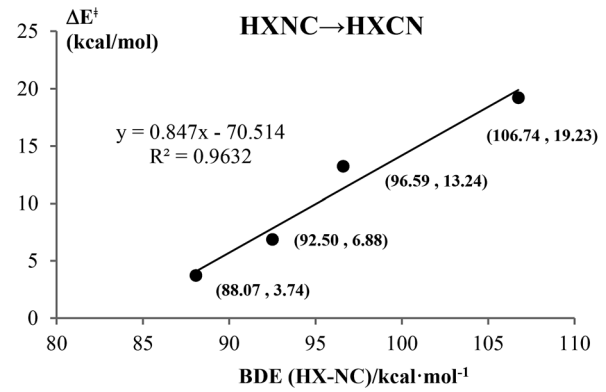

Fig. 8 The correlation between the bonding energies (HX–NC) and the barriers (HXNC → HXCN).

against fragments need to consume very high energies, as shown in Fig. 9 and 10.

c-XCHN ^{1}7 and c-XCNH ^{1}8

The two cyclic isomers c-XCHN 7 and c-XCNH **8** have singlet ground states, which have a XCN ring with the exocyclic CH and NH bonding in plane (see Fig. 13), respectively. ^{1}7 has much lower in energy than ^{1}**8** by 23.98 (X = Sn) and 22.52 (X = Pb) kcal mol^{-1}. The singlet PESs in Fig. 5 and 6 clearly show that ^{1}7 is kinetically stable due to the considerable rate-determining conversion barriers of 24.41 (Sn, ^{1}7 → ^{1}**2**) and 19.28 (Pb, ^{1}7 → ^{1}**11**) kcal mol^{-1}. However, ^{1}**8** possesses the much lower conversion barriers of 14.63 (Sn, ^{1}**8** → ^{1}**5**) and 11.30 (Pb, ^{1}**8** → ^{1}**9**) kcal mol^{-1}. Note that the kinetic stability of the hydrogenated c-XCN is much better than that of c-XCN.

Table 1 Spin density distribution (*s*) (in e) of c-XCN and the bond distances (*r*) (in Å)

MCN	*s*(X)	*s*(C)	*s*(N)	*r*(X–C)	*r*(X–N)	*r*(C–N)
c-CCN	0.400	0.400	0.200	1.58	1.30	1.30
c-SiCN	0.655	0.222	0.122	2.01	1.83	1.22
c-GeCN	0.843	0.087	0.070	2.22	1.99	1.20

Table 2 The binding energy (in kcal mol^{-1}) of the model carbene H_2X with BH_3 (as Lewis acid) and CO (as Lewis base)

X	The binding energy with BH_3	The binding energy with CO
Si	−44.18	−37.49
Ge	−34.86	−31.80
Sn	−21.23	−25.86
Pb	−13.29	−24.67

Agostic bonding in [H,Pb,C,N] system

For the singlet [H,Pb,C,N] system, we unexpectedly found three isomers ^{1}**9**, ^{1}**10** and ^{1}**11**, each of which possesses the unusual hydrogen bonding (see Fig. 14). In these structures, *r*(Pb–H) is between 2.20 and 2.30 Å and the ∠(X–H–C/N) is around 90°, which can be described as being associated with the agostic bonding.[30] Traditionally, the agostic bonding mainly exists between the transition metal and the hydrogen. Various roles have been found for agostic bonding, such as to weaken the C–H σ bonding in the organometallic reactions and to promote the easier hydrogen elimination.[31] However, there have been very limited reports concerning the involvement of main group metals in agostic bonding. Recently, the Sn and Pb agostic-type interactions have been reported, which can be a new method to stabilize the heavier group 14 carbene analogues.[32] In our work, the laboratory observation of the three [H,Pb,C,N] isomers ^{1}**9**, ^{1}**10** and ^{1}**11** seems unlikely due to the barriers of −2.67 kcal mol^{-1} (^{1}**9** → ^{1}**2**), −0.78 kcal mol^{-1} (^{1}**10** → ^{1}**8**) and −3.69 kcal mol^{-1} (^{1}**11** → ^{1}**2**). However, they provide non-negligible intermediates for the evolution of [H,Pb,C,N] system. Note that the agostic bonding cannot be found in the other four [H,X,C,N] systems (X = C, Si, Ge, Sn).

Laboratory and Astrophysical implications

It is of great to discuss the possible formation pathways of the Sn/Pb-containing species predicted in this work. It has been generally acknowledged that metal cyanides/isocyanides and hydrometal cyanides/isocyanides have a common origin, which can be formed by gas-phase reactions of X^+ or neutral metal in the very sparse interstellar or circumstellar clouds of dust (see Scheme 1).[33] We expect that various low-lying species RCN/RNC (R = H, HX; X = Sn, Pb) could be formed by the radiative association of X^+ with cyanopolyynes.

In laboratory, a rich knowledge of the [H,Si,C,N] isomers have been known. The chainlike HSiCN and HSiNC can be produced in the discharge of SiH_4 and C_2N_2 (HC_3N) mixtures.[4f] HCNSi can be generated during the condensation process of Si with HCN, then HSiCN, HSiNC, and c-SiCHN can be obtained by irradiation of the (silaisocyano)carbene HCNSi with visible or UV light.[4a] Accordingly, we optimistically anticipated that

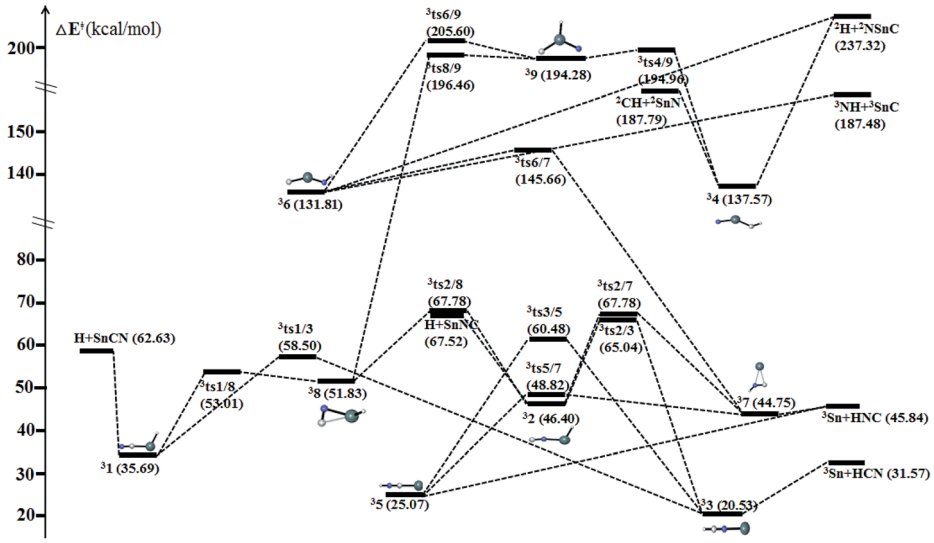

Fig. 9 Schematic potential energy surface of triplet [H,Sn,C,N] at the level of CCSD(T)/def2-QZVPP//B3LYP/def2-QZVPP + ZPVE in the parenthesis.

similar procedures could lead to generation of the analogous isomers of [H,X,C,N] (X = Sn/Pb). Combined with previous experimental synthesis studies and our potential energy surfaces analysis, we predicted that isomers XCN ^{2}**1**, XNC ^{2}**2**, HXCN ^{1}**1**, HXCN ^{1}**2**, HCNX ^{3}**3**, HNCX ^{3}**5**, c-XCHN ^{1}**7** and c-XCNH ^{1}**8** are potential candidates for future laboratory and astrophysical detection. Yet some isomers are meta-stable, and theirs detection could also be probable under the low-temperature conditions.

The vital metal-containing compounds are the metal cyanides/isocyanides and hydrometal cyanides/isocyanides in the circumstellar envelope. Due to significant challenges of the laboratory and interstellar detection, the detailed computational knowledge concerning the structural, isomerization and dissociation information of the rich potential energy surfaces of [X,C,N] and [H,X,C,N] in our work should thus give a very insightful assistance.

It has been usually considered that the mono-determinantal methodologies like DFT and/or CCSD(T) can be safely employed to treat various chemical systems.[34] Yet it should be of interest to evaluate the possibility of multiconfigurational character due to the involvement of Sn and Pb. To justify the reliability of the reported calculations, we applied the T1-diagnostic values from CCSD(T) calculations, which are presented in Table S4.† In most cases, the T1 diagnostic values are smaller than or around the recommended limit, *i.e.*, 0.02 for closed-shell systems[35] and

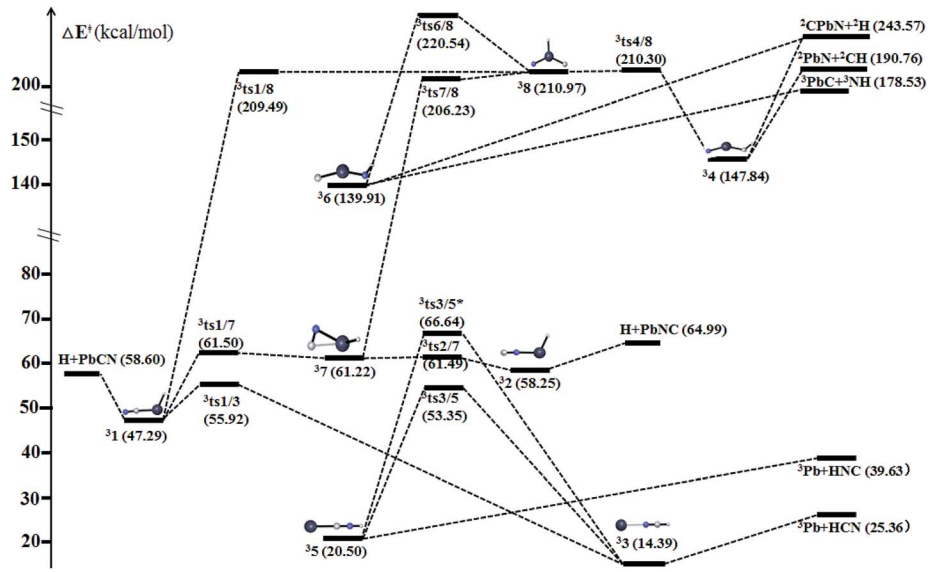

Fig. 10 Schematic potential energy surface of triplet [H,Pb,C,N] at the level of CCSD(T)/def2-QZVPP//B3LYP/def2-QZVPP + ZPVE in the parenthesis.

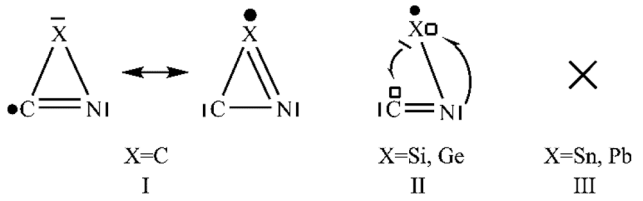

Fig. 11 Resonance structures of c-XCN: (I) X = C; (II) X = Si/Ge; (III) "×" represents "no" for X = Sn/Pb.

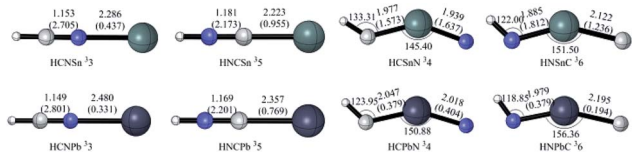

Fig. 12 Optimized geometries of isomers HCNX ^{3}**3**, HCXN ^{3}**4**, HNCX ^{3}**5** and HNXC ^{3}**6** (X = Sn, Pb) at the B3LYP/def2-QZVPP level. Bond lengths are in angstroms and angles are in degrees and the Mayer bond indices are in parentheses.

0.045 for open-shell systems.[36] However, for some structures with particularly high energies (and are much less of our interest), the T1 values are high and thus welcome future calculations based on the multiconfigurational methods. Most importantly, for the isomeric structures and the associated rate-determining transition states of the key isomers XCN ^{2}**1**, XNC ^{2}**2**, HXCN ^{1}**1**, HXCN ^{1}**2**, HCNX ^{3}**3**, HNCX ^{3}**5**, c-XCHN ^{1}**7** and c-XCNH ^{1}**8**, the T1 diagnostic values are reasonable.

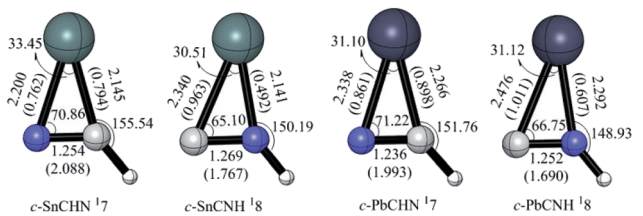

Fig. 13 Optimized geometries of isomers c-XCHN ^{1}**7** and c-XCNH ^{1}**8** (X = Sn, Pb) at the B3LYP/def2-QZVPP level. Bond lengths are in angstroms and angles are in degrees and the Mayer bond indices are in parentheses.

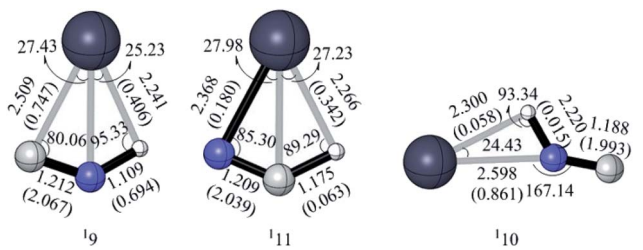

Fig. 14 Optimized geometries of isomers ^{1}**9**, ^{1}**10** and ^{1}**11** (X = Sn, Pb) at the B3LYP/def2-QZVPP level. Bond lengths are in angstroms and angles are in degrees and the Mayer bond indices are in parentheses.

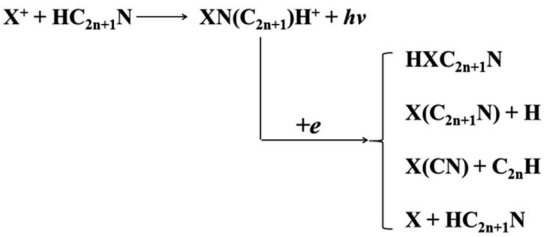

Scheme 1 The formation mechanism of metal cyanides/isocyanides and hydrometal cyanides/isocyanides.

Conclusions

A detailed potential energy surface study is performed on the completely unknown doublet/quartet [X,C,N] and singlet/triplet [H,X,C,N] (X = Sn/Pb) systems at CCSD(T)/def2-QZVPP//B3LYP/def2-QZVPP level. Isomers XCN ^{2}**1**, XNC ^{2}**2**, HXCN ^{1}**1**, HXCN ^{1}**2**, HCNX ^{3}**3**, HNCX ^{3}**5**, c-XCHN ^{1}**7** and c-XCNH ^{1}**8** are predicted to be potential candidates for future laboratory and interstellar detection. The calculated structures and spectroscopic properties are expected to stimulate future characterization of the metals cyanides/isocyanides and hydrometal cyanides/isocyanides both in laboratory and in interstellar space. The detailed isomerism of doublet/quartet [X,C,N] and singlet/triplet [H,X,C,N] (X = Sn/Pb) on PESs should be helpful for understanding the chemical evolution processes of these Sn, Pb-related isomers.

Conflicts of interest

There are no conflicts to declare.

Acknowledgements

This work was supported by the National Natural Science Foundation of China (No. 21773082, 21473069) and the "13th Five-Year" Scientific Planning Project of the Education Department of Jilin Province (No. JJKH20191000KJ). The two referees' invaluable comments and suggestions are greatly appreciated.

Notes and references

1 (*a*) J. Cernicharo and M. Guélin, *Astron. Astrophys.*, 1987, **183**, L10–L12; (*b*) P. J. Humphrey and D. A. Buote, *Astrophys. J.*, 2006, **639**, 136–156; (*c*) K. Matsushita, T. Ohashi and K. Makishima, *Publ. Astron. Soc. Jpn.*, 2000, **52**, 685–710; (*d*) S. Petrie, *Mon. Not. R. Astron. Soc.*, 1999, **302**, 482–490.

2 (*a*) M. Guélin, R. Lucas and J. Cernicharo, *Astron. Astrophys.*, 1993, **280**, L19–L22; (*b*) M. Guélin, S. Muller, J. Cernicharo, A. Apponi, M. McCarthy, C. Gottlieb and P. Thaddeus, *Astron. Astrophys.*, 2000, **363**, L9–L12; (*c*) M. Guélin, S. Muller, J. Cernicharo, M. McCarthy and P. Thaddeus, *Astron. Astrophys.*, 2004, **426**, L49–L52; (*d*) K. Kawaguchi, E. Kagi, T. Hirano, S. Takano and S. Saito, *Astrophys. J.*, 1993, **406**, L39–L42; (*e*) R. Pulliam, C. Savage, M. Agúndez, J. Cernicharo, M. Guélin and L. M. Ziurys, *Astrophys. J.*,

Lett., 2010, **725**, L181–L185; (*f*) B. Turner, T. Steimle and L. Meerts, *Astrophys. J.*, 1994, **426**, 97–100; (*g*) L. Zack, D. Halfen and L. M. Ziurys, *Astrophys. J., Lett.*, 2011, **733**, L36; (*h*) L. M. Ziurys, C. Savage, J. Highberger, A. Apponi, M. Guélin and J. Cernicharo, *Astrophys. J., Lett.*, 2001, **564**, L45–L48.

3 C. Cabezas, J. Cernicharo, J. L. Alonso, M. Agúndez, S. Mata, M. Guelin and I. Peña, *Astrophys. J.*, 2013, **775**, 133.

4 (*a*) G. Maier, H. P. Reisenauer, H. Egenolf and J. Glatthaar, *Eur. J. Org. Chem.*, 1998, 1307–1311; (*b*) M. McCarthy, C. Gottlieb and P. Thaddeus, *Mol. Phys.*, 2003, **101**, 697–704; (*c*) P. Redondo, C. Barrientos and A. Largo, *Astrophys. J.*, 2016, **828**, 45; (*d*) P. Redondo, C. Barrientos and A. Largo, *Astrophys. J.*, 2019, **871**, 180; (*e*) P. Redondo, A. Largo, Á. Vega-Vega and C. Barrientos, *J. Chem. Phys.*, 2015, **142**, 184301; (*f*) M. E. SANz, M. C. McCarthy and P. Thaddeus, *Astrophys. J., Lett.*, 2002, **577**, L71–L74; (*g*) M. Sun, A. Apponi and L. M. Ziurys, *J. Chem. Phys.*, 2009, **130**, 034309; (*h*) Q. Wang, Y. H. Ding, H. B. Xie and C. C. Sun, *J. Comput. Chem.*, 2006, **27**, 505–514; (*i*) Q. Wang, Y. H. Ding and C. C. Sun, *Chem. Phys.*, 2006, **323**, 413–428; (*j*) Z. X. Zhao, C. Y. Hou, X. Shu, H. X. Zhang and C. C. Sun, *Theor. Chem. Acc.*, 2009, **124**, 85–93.

5 (*a*) A. Endo, M. Ogasawara, A. Takahashi, D. Yokoyama, Y. Kato and C. Adachi, *Adv. Mater.*, 2010, **21**, 4802–4806; (*b*) H. Li, I. E. Castelli, K. S. Thygesen and K. W. Jacobsen, *Phys. Rev. B: Condens. Matter Mater. Phys.*, 2015, **91**, 045204; (*c*) K. Wu, Z. Yang and S. Pan, *Angew. Chem., Int. Ed. Engl.*, 2016, **55**, 6713–6715.

6 (*a*) Y. Kim, H. Noguchi and M. Amagai, *Microelectron. Reliab.*, 2006, **46**, 459–466; (*b*) C. Liu, C. Chen and K. Tu, *J. Appl. Phys.*, 2000, **88**, 5703–5709; (*c*) A. Mancini, P. Quadrelli, C. Milanese, M. Patrini, G. Guizzetti and L. Malavasi, *Inorg. Chem.*, 2015, **54**, 8893–8895; (*d*) E. Mosconi, P. Umari and F. De Angelis, *J. Mater. Chem. A*, 2015, **3**, 9208–9215.

7 (*a*) T. Chuang, L. Tsao, C. H. Chung and S. Chang, *Mater. Des.*, 2012, **39**, 475–483; (*b*) S. Ram, V. Kanchana, A. Svane, S. Dugdale and N. E. Christensen, *J. Phys.: Condens. Matter*, 2013, **25**, 155501.

8 (*a*) G. Merino, S. Escalante and A. Vela, *J. Phys. Chem. A*, 2004, **108**, 4909–4915; (*b*) M. Kaupp and P. V. R. Schleyer, *J. Am. Chem. Soc.*, 1993, **115**, 1061–1073.

9 K. Croswell, *Alchemy of the Heavens*, Anchor, 1996, ISBN 0-385-47214-5.

10 L. M. Hobbs, D. E. Welty, D. C. Morton, L. Spitzer and D. G. York, *Astrophys. J.*, 1993, **411**, 750–755.

11 (*a*) S. Van Eck, S. Goriely, A. Jorissen and B. Plez, *Nature*, 2001, **412**, 793; (*b*) D. Welty, L. Hobbs, J. Lauroesch, D. Morton and D. York, *Astrophys. J., Lett.*, 1995, **449**, L135.

12 M. J. Frisch, *et al.*, *Gaussian 09, Revision D.01*, Gaussian, Inc., Wallingford CT, 2009.

13 (*a*) Y. H. Ding, *GPESS*, Jilin University, Changchun, China, 2015; (*b*) F. F. He and Y. H. Ding, *RSC Adv.*, 2016, **6**, 26441; (*c*) X. X. Bo and Y. H. Ding, *GPESS version 1.0*, Jilin University, Changchun, China, 2018.

14 (*a*) C. Shao and Y. Ding, *Grid-Based Comprehensive Isomeric Search Algorithm*, Jilin University, Changchun, China, 2010; (*b*) X. X. Bo, H. F. Zheng, J. F. Xin and Y. H. Ding, *Chem. Commun.*, 2019, **55**, 2597–2600; (*c*) Z. H. Cui, M. Contreras, Y. H. Ding and G. Merino, *J. Am. Chem. Soc.*, 2011, **133**, 13228–13231; (*d*) X. Y. Tang, Z. H. Cui, C. B. Shao and Y. H. Ding, *Int. J. Quantum Chem.*, 2012, **112**, 1299–1306; (*e*) S. M. Gao and Y. H. Ding, *RSC Adv.*, 2012, **2**, 11764–11776; (*f*) C. Guo, Z. H. Cui and Y. H. Ding, *Int. J. Quantum Chem.*, 2013, **113**, 2213–2219; (*g*) C. Guo, Z. H. Cui and Y. H. Ding, *Struct. Chem.*, 2013, **24**, 263–270; (*h*) C. Guo, C. Wang and Y. H. Ding, *Struct. Chem.*, 2014, **25**, 1023–1031; (*i*) X. Y. Tang, Z. H. Cui, C. B. Shao and Y. H. Ding, *Int. J. Quantum Chem.*, 2012, **112**, 1299–1306; (*j*) J. F. Xin, X. R. Han, F. F. He and Y. H. Ding, *Front. Chem.*, 2019, **7**, 193; (*k*) J. Xu, X. Zhang, S. Yu, Y. H. Ding and K. H. Bowen, *J. Chem. Phys. Lett.*, 2017, **8**, 2263–2267; (*l*) Y. Y. Xue and Y. H. Ding, *Chem. Commun.*, 2019, **55**, 6373–6376; (*m*) Y. Y. Xue, J. J. Sui, J. Xu and Y. H. Ding, *ACS Omega*, 2017, **2**, 5407–5414; (*n*) X. Y. Zhang and Y. H. Ding, *Comput. Theor. Chem.*, 2014, **1048**, 18–24; (*o*) X. Y. Zhang and Y. H. Ding, *RSC Adv.*, 2015, **5**, 27134–27139; (*p*) H. F. Zheng, S. Yu, T. D. Hu, J. Xu and Y. H. Ding, *Phys. Chem. Chem. Phys.*, 2018, **20**, 26266–26272; (*q*) H. F. Zheng, J. Xu and Y. H. Ding, *J. Comput. Chem.*, 2019, **9999**, 1–10.

15 C. Peng and H. Bernhard Schlegel, *Isr. J. Chem.*, 1993, **33**, 449–454.

16 K. Fukui, *J. Phys. Chem.*, 1970, **74**, 4161–4163.

17 (*a*) J. Čížek, *Adv. Chem. Phys.*, 1969, 35–89; (*b*) G. D. Purvis III and R. J. Bartlett, *J. Chem. Phys.*, 1982, **76**, 1910–1918; (*c*) G. E. Scuseria, C. L. Janssen and H. F. Schaefer III, *J. Chem. Phys.*, 1988, **89**, 7382–7387; (*d*) G. E. Scuseria and H. F. Schaefer III, *J. Chem. Phys.*, 1989, **90**, 3700–3703.

18 C. Adamo, G. E. Scuseria and V. Barone, *Chem. Phys. Lett.*, 1999, **111**, 2889–2899.

19 (*a*) A. Schäfer, H. Horn and R. Ahlrichs, *J. Chem. Phys.*, 1992, **97**, 2571–2577; (*b*) F. Weigend, F. Furche and R. Ahlrichs, *J. Chem. Phys.*, 2003, **119**, 12753–12762; (*c*) D. Feller, *J. Comput. Chem.*, 1996, **17**, 1571–1586; (*d*) K. L. Schuchardt, B. T. Didier, T. Elsethagen, L. Sun, V. Gurumoorthi, J. Chase, J. Li and T. L. Windus, *J. Chem. Inf. Model.*, 2007, **47**, 1045–1052.

20 D. K. Lee, I. S. Lim, Y. S. Lee and G. H. Jeung, *Int. J. Mass Spectrom.*, 2008, **271**, 22–29.

21 I. Mayer, *Chem. Phys. Lett.*, 1983, **97**, 270–274.

22 K. B. Wiberg, *Tetrahedron*, 1968, **24**, 1083–1096.

23 T. Lu and F. Chen, *J. Theor. Comput. Chem.*, 2012, **11**, 163–183.

24 T. Lu and F. Chen, *J. Comput. Chem.*, 2012, **33**, 580–592.

25 (*a*) A. Sekiguchi, R. Kinjo and M. Ichinohe, *Science*, 2004, **305**, 1755–1757; (*b*) L. Pu, B. Twamley and P. P. Power, *J. Am. Chem. Soc.*, 2000, **122**, 3524–3525; (*c*) A. D. Phillips, R. J. Wright, M. M. Olmstead and P. P. Power, *J. Am. Chem. Soc.*, 2002, **124**, 5930–5931; (*d*) M. Stender, A. D. Phillips, R. J. Wright and P. P. Power, *Angew. Chem., Int. Ed.*, 2002, **41**, 1785–1787.

26 W. M. Haynes, *CRC handbook of chemistry and physics*, CRC press, 2014.

27 (*a*) G. A. Garcia, J. Krüger, B. Gans, C. Falvo, L. H. Coudert and J. C. Loison, *J. Chem. Phys.*, 2017, **147**, 013908; (*b*) A. Mebel and R. Kaiser, *Astrophys. J.*, 2002, **564**, 787.

28 (*a*) J. Flores, *Chem. Phys.*, 2005, **310**, 303–310; (*b*) Q. Wang, Y. H. Ding and C. C. Sun, *J. Chem. Phys.*, 2005, **122**, 204305.

29 (*a*) A. Largo-Cabrerizo, *Chem. Phys. Lett.*, 1988, **147**, 95–98; (*b*) M. McCarthy, A. Apponi, C. Gottlieb and P. Thaddeus, *J. Chem. Phys.*, 2001, **115**, 870–877; (*c*) N. A. Richardson, Y. Yamaguchi and H. F. Schaefer III, *J. Chem. Phys.*, 2003, **119**, 12946–12955.

30 J. Saßmannshausen, *Dalton Trans.*, 2012, **41**, 1919–1923.

31 (*a*) P. J. Chirik, N. F. Dalleska, L. M. Henling and J. E. Bercaw, *Organometallics*, 2005, **24**, 2789–2794; (*b*) M. Etienne, R. Mathieu and B. Donnadieu, *J. Am. Chem. Soc.*, 1997, **119**, 3218–3228; (*c*) N. Koga, S. Obara, K. Kitaura and K. Morokuma, *J. Am. Chem. Soc.*, 1985, **107**, 7109–7116; (*d*) L. H. Shultz and M. Brookhart, *Organometallics*, 2001, **20**, 3975–3982.

32 (*a*) K. Izod, W. McFarlane, C. Wills, W. Clegg and R. W. Harrington, *Organometallics*, 2008, **27**, 4386–4394; (*b*) K. Izod, C. Wills, W. Clegg and R. W. Harrington, *Organometallics*, 2009, **28**, 2211–2217.

33 (*a*) R. C. Dunbar and S. Petrie, *Astrophys. J.*, 2002, **564**, 792; (*b*) S. Petrie, *Mon. Not. R. Astron. Soc.*, 1996, **282**, 807–819.

34 R. Grande-Aztatzi, J. L. Cabellos, R. Islas, I. Infante, J. M. Mercero, A. Restrepo and G. Merino, *Phys. Chem. Chem. Phys.*, 2015, **17**, 4620–4624.

35 T. J. Lee and P. R. Taylor, *Int. J. Quantum Chem.*, 1989, **36**, 199–207.

36 (*a*) J. C. Rienstra-Kiracofe, W. D. Allen and H. F. Schaefer, *J. Phys. Chem. A*, 2000, **104**, 9823; (*b*) S. R. Miller, N. E. Schultz, D. G. Truhlar and D. G. Leopold, *J. Chem. Phys.*, 2009, **130**, 024304.

